

# Electron Diffraction and $^{47,49}\text{Ti}$ and $^{17}\text{O}$ NMR Studies of Natural and Synthetic Brookite

T. J. Bastow,<sup>†</sup> G. Doran,<sup>†</sup> and H. J. Whitfield<sup>\*,†,‡</sup>

Division of Manufacturing Science and Technology, CSIRO, Private Bag 33, Rosebank MDC, Clayton, Victoria 3169, Australia, and Department of Applied Physics, RMIT, Box 2476V, Melbourne, Victoria 3001, Australia

Received August 2, 1999. Revised Manuscript Received November 30, 1999

Brookite,  $\text{TiO}_2$ , synthesized by hydrothermal processing of a titanium oxide gel was shown by powder X-ray and single-crystal electron diffraction to consist of very well ordered single crystals. The titanium coupling constant determined from  $^{47,49}\text{Ti}$  NMR spectroscopy is intermediate between the coupling constants for anatase and rutile.  $^{17}\text{O}$  NMR spectroscopy locates the two crystallographically inequivalent oxygen atoms in brookite. Electron diffraction and microscopy and Ti NMR show that a comparison sample of naturally occurring brookite has many more defects.

## Introduction

The structure and properties of the anatase and rutile polymorphs of titanium dioxide have been intensively studied because of their industrial importance. The existence of these two polymorphs has allowed a convenient comparison of the accuracy and structural sensitivity of energy-level calculations with observations of X-ray absorption<sup>1</sup> and electron energy-loss<sup>2</sup> spectra. The existence of a third polymorph of titanium dioxide, namely brookite, has been utilized rather less in such studies possibly due to the lack until recently of a well-characterized method of synthesis and the high level of impurities, chiefly Fe and Nb, that are found in many mineral deposits of brookite.<sup>3</sup>

Brookite was reported to have been synthesized in the 19th century, but most of these synthetic preparations were not well-characterized.<sup>3</sup> Synthesis of titanium oxide at low temperatures by sol–gel techniques usually yields anatase, which inverts to rutile on heating.<sup>4</sup> A recent sol–gel synthesis of nanocrystalline anatase followed by hydrothermal treatment was shown by high-resolution transmission electron microscopy to contain domains of brookite.<sup>5</sup> Such a mixed phase is possibly typical of many, if not most, of the reported procedures for brookite synthesis. However, one reported synthesis of brookite using an alternative hydrothermal procedure<sup>6</sup> gives a single-phase, well-crystallized, product.

In the present work, we report on comparison of brookite synthesized by this latter method with a

mineral sample of brookite, using the techniques of selected area and convergent beam electron diffraction, electron microscopy, and  $^{47,49}\text{Ti}$  and  $^{17}\text{O}$  nuclear magnetic resonance.

## Experimental Section

A  $\text{TiO}_2$  gel, prepared by hydrolysis of a titanium alkoxide, was crystallized under hydrothermal conditions<sup>6</sup> in the presence of sodium hydroxide to give brookite.

A mineral sample of brookite, No M12710, kindly supplied by the Department of Mineralogy and Petrology of the Museum of Victoria, was crushed and separated from a quartz matrix by hand selection. This sample originally from Magnet Cove, Arkansas, was black to reflected light but transparent in thin sections.

X-ray powder diffraction patterns of the natural and synthetic brookite were collected on a Siemens D-500 diffractometer using nickel-filtered  $\text{Cu K}\alpha$  radiation and a graphite monochromator.

Selected area and convergent beam electron diffraction (CBED) patterns and electron micrographs were recorded on an analytical JEOL 2010 electron microscope with a  $\text{LaB}_6$  source. Lightly crushed samples crystals were dispersed with ethanol on to carbon film-covered copper grids and dried in an air oven before insertion into the microscope. The microscope is provided with an EDS attachment that allowed chemical analysis of samples.

The NMR spectra were obtained using a Bruker MSL 400 spectrometer with a nominal field of 9.395 T. For the  $^{47,49}\text{Ti}$  spectrum, a probe with a 10 mm transverse coil was used at an operating frequency of 22.608 MHz. The spectrum was obtained using a two-pulse echo sequence where the whole echo was collected and Fourier transformed, and the modulus taken to give the absorption line shape; approximately 500 000 transients were collected. The pulse width was 5  $\mu\text{s}$ , which excited and detected a frequency region of 250 kHz. The pulse sequence repetition time was 0.1 s. The spectrum was referenced to  $\text{SrTiO}_3$  at zero shift. For the  $^{17}\text{O}$  spectrum, a MAS probe was employed with a 4 mm silicon nitride rotor and a spinning frequency of 10 kHz. A single-pulse phase-cycled sequence was used with a repetition time of 5 s; approximately 10 000 transients were collected. The reference was water at zero shift.

(7) Pauling, L.; Sturdivant, J. H. *Z. Kristallogr.* **1928**, *68*, 239.

\* To whom correspondence should be addressed. E-mail: harold.whitfield@rmit.edu.au.

<sup>†</sup> CSIRO.

<sup>‡</sup> RMIT.

(1) Laan, G. van der, *Phys. Rev. B* **1990**, *41*, 12366.

(2) Brydson, R.; Sauer, H.; Engel, W.; Hofer, F. *J. Phys. Condens. Matter* **1992**, *4*, 3429.

(3) Deer, W. A.; Howie, R. A.; Zussman, J. *Rock Forming Minerals*, Longmans: London, 1962; p 44.

(4) Bastow, T. J.; Moodie, A. F.; Smith, M. E.; Whitfield, H. J. *J. Mater. Chem.* **1993**, *3*, 697.

(5) Penn, R. L.; Banfield, J. F. *Am. Miner.* **1998**, *83*, 1077.

(6) Keesman, I. *Z. Anorg. Allg. Chem.* **1966**, *346*, 30.

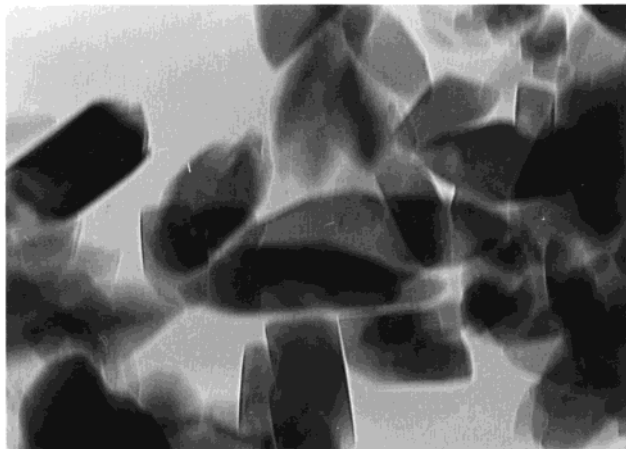


**Figure 1.** Electron micrograph of synthetic brookite crystals showing crystal size and morphology. The scale is  $1 \mu\text{m} = 500 \text{ nm}$ .

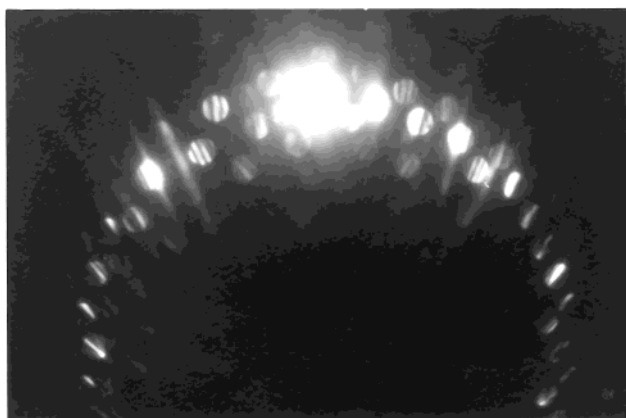


**Figure 2.** Convergent beam electron diffraction of synthetic brookite tilted slightly from a zone to a Laue circle. Note detail in diffracted beams and Kikuchi bands.

### Results and Discussion

Powder X-ray diffraction of synthetic brookite gave extremely sharp lines with no detectable second phase present.

Low-magnification electron microscope images of the synthetic specimen showed it consists of fairly uniform size acicular crystals. (Figure 1). The diffraction pattern taken, with a highly collimated electron beam, of a selection of randomly oriented crystals showed dynamic shape-function–structure; for crystals in the right orientation, several orders of diffraction were observed. This indicates that the crystallites are perfect, are highly crystalline, and have well-developed facets. High-resolution electron microscopy images gave one-dimensional lattice images that showed no evidence of stacking faulting or disorder. The sample was extremely stable even in a focused electron beam and CBED patterns were obtained from individual crystals. A CBED pattern of one crystal in a Laue circle orientation (Figure 2) shows strong Kikuchi bands and detail in the diffracted beams typical of a well-ordered single crystal. The manipulation of the crystals to obtain zone axis CBED patterns and two-dimensional lattice images was not easy because of their small size nor could large angle CBED patterns be obtained.

The mineral specimen of brookite also proved to be extremely stable in the microscope electron beam and

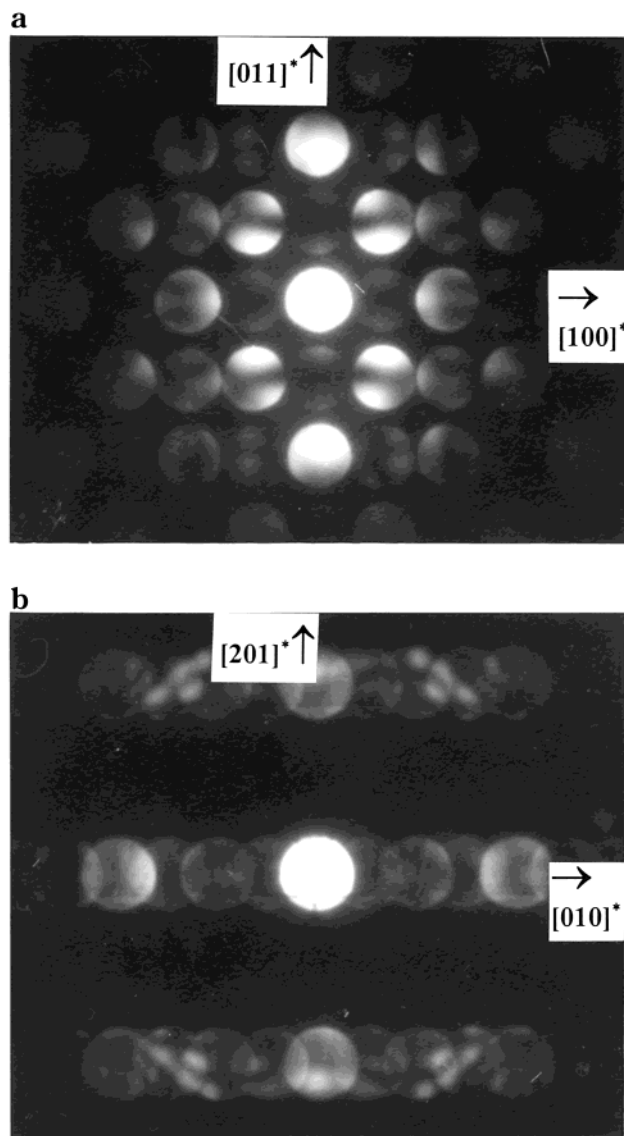


**Figure 3.** Convergent beam electron diffraction of natural brookite (a) with incident beam along  $[011]$  showing GM bands for  $h00$  beams with  $h$  odd and (b) with incident beam along  $[102]$  showing GM bands on  $0k0$  beams for  $k = 2n$ .

selected area, and both normal and large-angle CBED patterns and electron micrographs were obtained for a number of projections. These were in good accord with the space group<sup>7</sup> and dimensions of the crystals, namely, orthorhombic space group  $Pcab$  (no. 61) with unit cell dimensions  $a = 5.456$ ,  $b = 9.182$ , and  $c = 5.143 \text{ \AA}$ . This space group projects, down all three principal axes, into the space group  $pgm$ , and in the first Born approximation, the  $h00$  reflections are forbidden for  $h = 2n + 1$ , the  $0k0$  is forbidden for  $k = 2n + 1$ , and the  $00l$  is forbidden for  $l = 2n + 1$ .

Observations by diffraction or microscopy revealed numerous crystal imperfections such as stacking faults and dislocations. However, by observation of numerous crystals, some were selected that had well-ordered regions that showed the symmetry elements of the brookite structure. In a CBED pattern of natural brookite taken with the incident beam along the  $[011]$  direction (Figure 3a), the  $h00$  scattered beams with  $h$  odd are weak and show GM bands. Similarly, when the incident beam is along the  $[102]$  direction (Figure 3b),

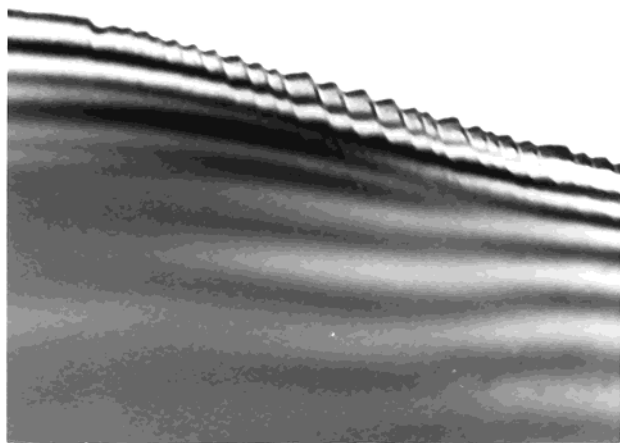


**Figure 4.** Electron micrograph of natural brookite crystal showing stepped surface. The scale is 1 mm = 6.3 nm.

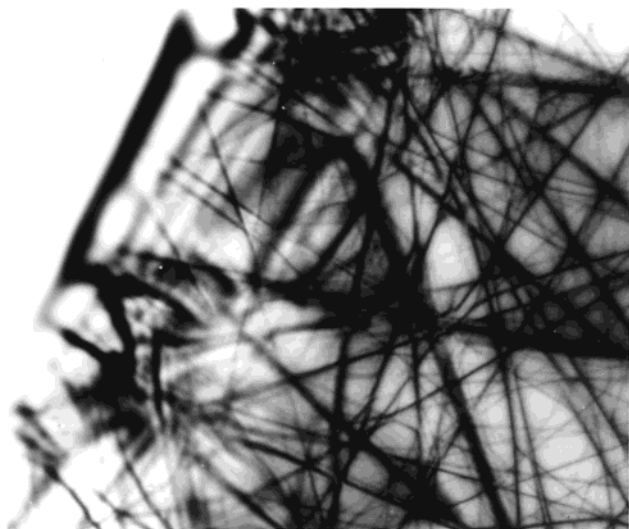


**Figure 5.** LACBED pattern of a crystal of natural brookite with incident beam along the [412] direction.

the  $0k0$  scattered beams with  $k$  odd are weak and show GM bands as well.

In an electron micrograph (Figure 4) taken with the incident electron beam along the [011] direction of a dislocation-free region of crystal, the surface shows serrated edges. Such behavior has been reported for molecularly clean surfaces of oxides of magnesium oxide<sup>8</sup> and zirconium oxide.<sup>9</sup> A nominal surface that would be highly polar actually consists of steps of unit cell dimension exposing nonpolar surfaces.<sup>10</sup> Also observed in bright- and dark-field images of an adjacent region of this crystal were faults that appeared to indicate planer stacking faults. Where these faults intersected, the crystal surface dislocations were observed parallel to the incident electrons. The presence of numerous crystal defects in the mineral sample meant there were few sufficiently large and well-ordered regions of crystal to obtain good large-angle convergent beam patterns. The pattern of Figure 5 is taken with the incident beam along the [412] direction of a wedge-

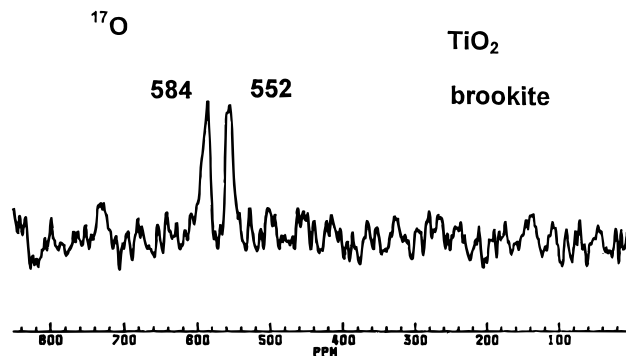


**Figure 6.**  $^{17}\text{O}$  NMR spectrum of synthetic brookite.

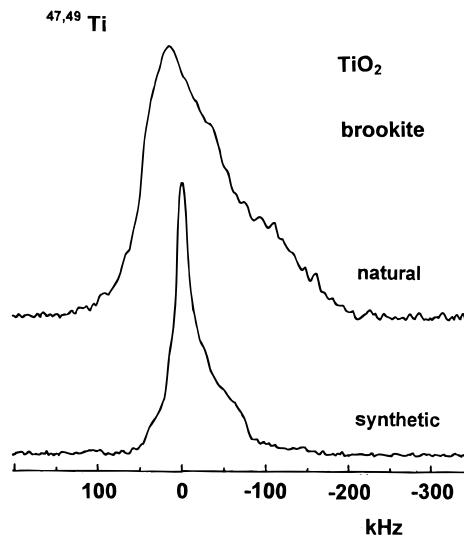


**Figure 7.**  $^{47,49}\text{Ti}$  NMR spectrum of synthetic and natural samples of brookite.

shaped crystal. Dislocations can be seen interacting with the pendellosung near the edge of the crystal.

A number of crystals were examined by EDS. The only cations, other than Ti, observed in the crystals were Nb and Fe. From the intensity of EDS peaks, the Nb content was estimated as about 1% and the Fe content as about 0.5%. These are the elements commonly found in natural brookite, although often in much higher amounts.<sup>11</sup>

The  $^{17}\text{O}$  NMR of synthetic brookite is shown in Figure 6, and its  $^{47,49}\text{Ti}$  NMR is shown in Figure 7. These spectra may be compared with spectra from anatase and rutile. The crystal structure of brookite shows that as in anatase and rutile each titanium is surrounded by an octahedral group of oxygen atoms and each oxygen is coordinated by three titanium atoms. The three polymorphs of  $\text{TiO}_2$  differ in the mutual arrangement of the oxygen octahedra.

Brookite is orthorhombic with two crystallographically inequivalent O sites and one Ti site, all of which lack axial symmetry. In the  $^{17}\text{O}$  NMR spectrum of the synthetic brookite (Figure 6), the two sites are well-resolved and have approximately equal intensity. As for anatase and rutile with oxygen in natural abundance, MAS is sufficiently efficient that, with the observed signal-to-noise ratio, it is not possible to detect any quadrupolar detail in the spectrum. The shift values for

(8) Moodie, A. F.; Warble, C. E. *Mater. Sci. Res.* **1975**, *10*, *Sintering and Catalysis*; Kuczynski, G. C., Ed.; Plenum: New York, 1975; p 1.

(9) Warble, C. E. *Ultramicroscopy* **1984**, *15*, 301.

(10) Burton, N. K.; Cabrera, N.; Frank, F. C. *Philos. Trans. A* **1951**, *243*, 299.

(11) *U.S. Natl. Bur. Stand. Monogr.* **1964**, *25*, (3) 57.

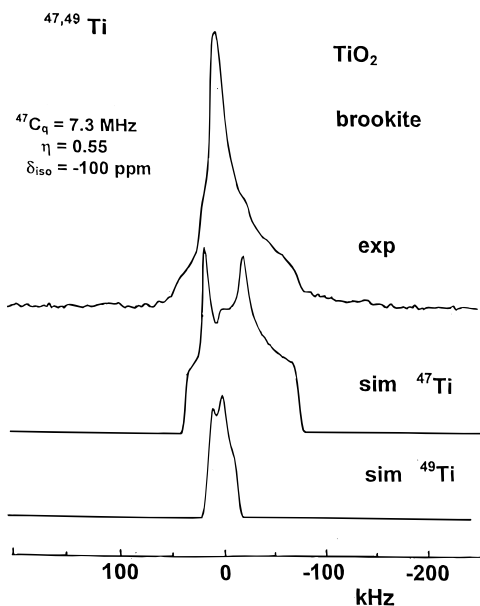


**Figure 8.** Observed and simulated  $^{47}\text{Ti}$  NMR spectra of synthetic brookite.

the two O sites,  $\delta_{\text{high}}$  and  $\delta_{\text{low}}$ , are relatively similar to the single-site values of anatase and rutile. The  $\delta_{\text{high}}$  value is particularly close to, although distinct from, that in rutile. The  $^{17}\text{O}$  NMR lines are very sharp, reflecting the perfection and freedom from defects of the crystals. The preparation is clean brookite, with no trace of anatase or rutile present.

The  $^{47,49}\text{Ti}$  NMR spectrum of synthetic brookite (Figure 7) is much sharper than the comparison spectrum previously reported<sup>12</sup> from a geological sample of

**Table 1**

TiO <sub>2</sub> polymorph	$^{47}\text{C}_q$ (MHz)	$\eta$	$^{47}\delta_{\text{iso}}$ (ppm)	$^{17}\delta_{\text{iso}}$ (ppm)
anatase <sup>a</sup>	5.85 (0.02)	0	0 (20)	557
rutile <sup>a</sup>	17.0 (0.05)	0.19 (0.02)	-195 (20)	596.5
brookite <sup>b</sup>	7.3 (0.05)	0.55 (0.05)	-100 (20)	552 584

<sup>a</sup> References 4 and 12. <sup>b</sup> Present work.

brookite that lacks detail and is much broader. Interpretation of the spectrum of synthetic brookite is that the sharp central feature is unresolved  $^{49}\text{Ti}$ , and the broad component (simulated in Figure 8) is from  $^{47}\text{Ti}$ . The simulated value of  $^{47}\text{C}_q = 7.3$  MHz is intermediate between that of anatase and rutile. The asymmetry of the EFG ( $\eta = 0.55$ ) is higher than that in rutile ( $\eta = 0.19$ ) or anatase ( $\eta = 0$ ). The nuclear hyperfine details for the three TiO<sub>2</sub> polymorphs are collected in Table 1.

The method of synthesis of brookite according to Keesman<sup>6</sup> gives a highly ordered crystalline product and modifications of the synthesis are planned with the objective of obtaining larger crystals and crystals doped with other cations.

**Acknowledgment.** We thank Dermot Henry of the Museum of Victoria for the brookite mineral, Natasha Rockelman for X-ray powder patterns, Terry Turney for helpful discussions, and Florence Babonneau for directing our attention to the work by Keesman.<sup>6</sup>

CM990486M

(12) Bastow, T. J. *Solid State NMR* **1998**, *12*, 201.